Analysis of Magnetic Degradation and Kerf Surface for NO20 Non-Oriented Electrical Steel Subjected to Remote Laser Cutting

Daniele De Gaetano[1], *Member, IEEE*, Alexei Winter[1], Lloyd Tinkler[1],
and Xiao Chen[2], *Senior Member, IEEE*
[1] Advanced Manufacturing Research Centre (AMRC), The University of Sheffield, Sheffield, S60 5TZ, UK
[2] School of Electrical and Electronic Engineering, The University of Sheffield, Sheffield, S1 4DT, UK

This article investigates process parameters for remote laser cutting of non-grain-orientated silicon iron electrical steel (NO20), targeting a precise and clean lamination surface, acceptable overall cutting time and low degradation of magnetic properties. NO20 is commonly used in rotating electrical machines. Remote laser cutting offers a higher design flexibility with respect to traditional cutting methods such as punching, resulting in higher design freedom. However, incorrect laser settings can result in a strong degradation of material magnetic properties as well as burned lamination surfaces and inaccurate cut profiles. Optimal laser power and scan speed settings are identified by microscopy of partial cuts and by surface inspections of fully cut sample strips. In addition, the magnetic characterisation of sample strips is carried out to identify the optimum idle time between scans. Finally, the optimum parameter set for remote laser cutting investigated within the study is then compared against guillotine and electrical discharge machining (EDM) methods, and found to compare favorably in terms of cut quality and impact on magnetic properties.

***Index Terms*—Soft magnetic materials, laser cutting, microscopy analysis, magnetic characterisation.**

I. Introduction

Soft magnetic materials are the core of electromagnetic devices such as electrical machines. Several alloys, commonly silicon-iron, nickel-iron and cobalt-iron, can be used for different applications [1]. All manufacturing processes result in deterioration to some degree, and therefore there is a growing interest in understanding and minimising the impact of manufacture on the materials. Indeed, the cutting process can strongly affect the magnetic material performance as well as offering different levels of mechanical accuracy. Different methods are used for lamination cutting such as guillotine, punching, photo-corrosion, electrical discharge machining (EDM), fusion laser and remote laser, all with their pros and cons.

The remote laser cutting technique allows a relative motion between the work piece and laser by beam manipulation with a Galvanometer scanner. The process produces a mix of molten and vaporised material in the processed area. The vaporisation causes the molten material to be ejected from the kerf [2]. Remote laser cutting offers a lower cycle time compared with the traditional fusion laser technique. Authors in [3] show how the cycle time is reduced by 2/3 on medium complexity tooth geometries. The same reference proposes a magnetic comparison on M235 35A lamination with width of 5 mm at 50 Hz, showing how an ultra-short pulse (picoseconds order) laser presents the better performance in terms of relative permeability (up to 1.5 T) with respect to continuous-wave remote laser, guillotine, punching and solid-state fusion laser. After 1.5T, the ultra-short pulse laser and continuous-wave remote laser are comparable presenting slightly better values with respect to the last other techniques. The same conclusions can be extended to lower specific losses as well. Moreover, it is shown how the power reduction and idle time settings of the remote laser can help to preserve the original magnetic characteristic of the material.

The impact on the magnetic performance in 2% silicon non-oriented alloy material of four different techniques, guillotine, punching, fusion laser and photo-corrosion, and with and without annealing treatment was investigated in [4]. After cutting, the annealing procedure helps to reduce losses and increase the permeability for all the cutting techniques except in the case of photo-corrosion. Annealing improves strongly the permeability for the samples cut by fusion laser by 22.6%.

Authors in [5] demonstrated that after a threshold point the increment of cutting speed does not have a significant impact on the depth of groove. The increment of cutting speed deals with a reduction of geometry accuracy. Burr height is reduced with increasing scan speed, although this phenomenon strongly depends on characteristics of the material.

In [6], authors compare CO_2 fusion laser, remote laser and remote fusion laser in terms of accuracy and heat affected zone (HAZ). The remote fusion laser does not use the beam to vaporise the molten material from the kerf surface as the remote laser, but the material removal is by melting only, carried away by the high-pressure assist gas from the bottom surface of the material. The comparison shows a larger HAZ for the remote fusion laser with respect to the CO_2 fusion laser and remote laser.

In [7], authors mention the issue of separating the cut portion from the rest of the lamination for conventional remote laser technologies. This can sometimes be problematic, due to the fact that the molten material is not fully ejected from the narrow kerfs and remains, connecting the two pieces.

In [8], the effects of laser cutting were studied and an improved model for considering the losses by manufacturing

Corresponding author: Daniele De Gaetano (e-mail: d.degaetano@sheffield.ac.uk). "This work is supported by the U.K. EPSRC through research award EP/S018034/1.

was carried out, finding a maximum difference of 14% in the core AC losses between not-included cutting effects and included cutting effects. The laser topology was not specified in the paper, mentioning only that the laser cutting was performed for small-scale production of machines in industry.

The punching effects on electrical sheets were investigated in [9] based on measurement of strips of sheets with various widths on an enlarged Epstein frame and proposing a design of a permanent magnet machine. Authors have found that the optimal design with a not-included deterioration under-estimates the stator core losses by 175% which leads to an underestimation of 5^o C in the temperature of windings.

The paper [10] compares the microstructure and magnetic properties of punched electrical steel before and after annealing with an improvement of core losses up to 37%.

An improved model to include the manufacturing effects at the design stage was proposed in [11] where cutting, welding and shrink fitting effects were included.

This work seeks to identify optimum cutting parameters for non-grain-oriented (NGO) silicon-iron NO20 laminations by a continuous-wave remote laser. Partial cuts by a single beam, with various laser power (P) and speed (S) settings, are made in order to study the cut uniformity and cleanliness with a single beam scan. Using microscopy of the partial cuts, cut depth is measured, which also allows the number of scans required to cut through the entire thickness to be estimated. Based on the microscopy analysis, baseline settings were selected. Several fully cut samples using the optimum laser power and speed working point are produced with different laser idle time (IT) between scans. The trend of degradation of magnetic properties versus idle time is investigated. Finally, a comparison of remote fibre laser against guillotine and EDM cuttings is proposed.

II. Equipment, material, and proposed methodology

A. Experimental equipment and material under test

An SPI lasers RedPower Qube 2 kW fibre laser is used for both partially and fully cutting the material with different setting of power, speed and idle time between beam scans. The mentioned laser presents the following characteristics: wavelength 1075±2 nm, maximum power 2 kW, maximum switching frequency 50 kHz, fibre diameter 25 μm. The laser system is completed by a collimator (PiPA-Q,f114), galvanometer (Raylase superScan IV) with a field of view of 85 mm x 85 mm and a maximum scan speed of 8000 mm/s, and a motion system (Aerotech Infinite Field of View) with an overall field of view of 600 mm x 600 mm.

The microscope Alicona μCMM is used to analyse the single scan samples for different settings of power and speed. A simple USB microscope is used to capture the kerf surface of the fully cut samples.

The Laboratorio Elettrofisco AMH-1K-S permeameter and ST-100 tester are used to characterise the magnetic proprieties of fully cut single lamination strips. The material under test is the NO20. It is a NGO electric steel made by Tata steel. This silicon-iron lamination presents the following physical and mechanical properties: electrical resistivity at 23^{o}C = 59 $\mu\Omega$ cm; thermal conductivity at 23^{o}C = 21 W/(m K); Young's modulus = 185 GPa; density (assumed) = 7.60 kg/dm^3. The main NO20 material magnetic properties by data sheet are: specific total loss at 1 T and 50 Hz = 1.05 W/kg; specific total loss at 1.5 T and 50 Hz = 2.40 W/kg; specific total loss at 1 T and 400 Hz = 12.1 W/kg; specific total loss at 1.5 T and 400 Hz = 27.9 W/kg; the peak magnetic polarisation is 1.57 T at 2500 A/m and 50 Hz ; the peak magnetic polarisation is 1.77 T at 10000 A/m and 50 Hz.

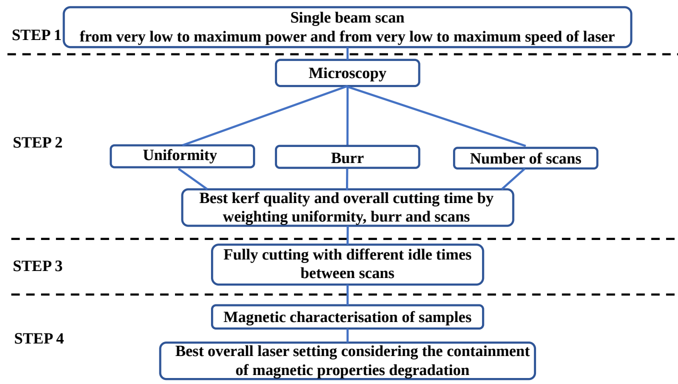

Fig. 1: Process for the optimum mechanical and magnetic lamination cutting by laser.

B. Proposed methodology

The process of selecting the optimum remote fibre laser working point considering the overall cutting time, cutting quality and magnetic properties is proposed in Fig. 1. The uniform cutting criterion was selected as the most important parameter, followed by burr analysis, and the number of scans to fully cut the material. Performing single beam scans, from very low power to the maximum power (2 kW), and from low speed to maximum speed, is the first step. The second step is to perform a microscopy analysis to investigate about a good trade-off, weighting uniformity, number of scans, and material accumulation around the kerf surface (burr). The third step is to fully cut the samples with different idle times between scans which could have an impact on the magnetic properties of the material. It is worth highlighting that the effective time between beam scans is the idle time plus the time for completing the cut path. The final step is to magnetically characterise the samples, analysing the impact of the laser IT (time between two scans) on the material magnetic properties.

III. Optimum cutting laser settings

This section finds acceptable remote laser settings from the cutting quality point of view, considering the overall cutting time, for NO20 electric steel material. The good trade-off point is selected by microscopy analysis performed on several partial cuttings (single beam scan) using a range of laser power and speed settings. The selection of the baseline point is based on different criteria such as cutting uniformity, number of scans and burr. The production of several fully cut samples, using the selected baseline point settings for the laser, are produced with different idle times. Those samples will be fully magnetically characterised (section IV).

A. Beam single scan

Several single beam scans, for the partial cuttings of the NO20 material, are performed. The full list is presented in table I.

Power [kW]	5 [m/s]	6 [m/s]	7 [m/s]	8 [m/s]
0.25	x	x	x	x
0.50	x	x	x	x
0.75	x	x	x	x
1.00	x	x	x	x
1.25	x	x	x	x
1.50	x	x	x	x
1.75	x	✓	x	✓
2	x	✓	x	✓

TABLE I: Laser settings - x indicates not satisfactory results; ✓ indicates satisfactory results.

The power (P) setting varies from 0.25 kW to 2.00 kW with a step of 0.25 kW, while the speed (S) from 5 m/s to 8 m/s with a step of 1 m/s. The single partial cuttings are analysed via microscopy. The scans were 20 mm long. The material removal analysis is carried out on the cross-section. The μCMM microscope produces depth information which allows to analyse the kerf depth. Those points are scanned at three points along the sample at 5 mm intervals.

The selection of the best setting point is based on the following three criteria:

1) Uniformity of cutting
2) Burr (material accumulation around edge of the kerf, rising higher that the original surface)
3) Number of scans

Fig. 2 shows depth profile, extracted from the μCMM, cuttings by single beam scans for the settings which have a good uniformity and consistent material removal only. Additionally, it shows the sample sketch, with partial cutting and analysed areas. It is clear as all of those settings have a good uniformity in terms of partial cutting between bottom, middle and top. Analysing the material accumulation around the kerf surface (burr), it is possible to appreciate the good quality of cutting with all four setting points. It is possible to see that the highest value is 27 μm for P=1.75 kW S=6 m/s (top), 28 μm for P=1.75 kW S=8 m/s (middle), 20 μm for P=2 kW S=6 m/s (top), and 21 μm for P=2 kW S=8 m/s (middle). Analysing the number of scans, thus the cutting time, the best options are the two with a speed of 6 m/s. In both cases, four single beam scans are enough fully cut through the material thickness. Indeed, the NO20 thickness is 0.20 mm and the less deep material removal with a single scan is 53 μm for P = 1.75 kW and 51 μm for P = 2 kW, respectively. The number of scans is calculated by a ratio between material thickness and the cut depth. The assumption is that the depth of cutting increases linearly with the number of scans.

In order to select the best laser setting point, the 3 different criteria are evaluated and scored. The values that can be assigned to uniformity, burr, and number of scans range from

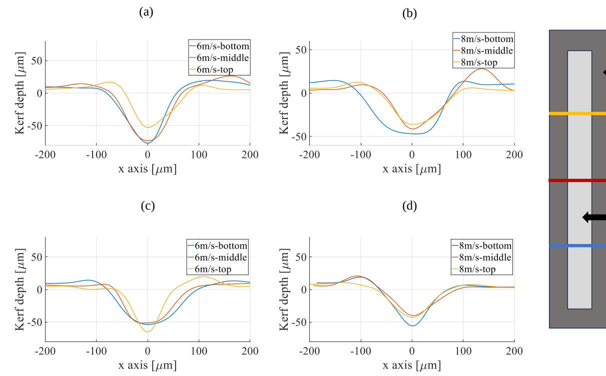

Fig. 2: Kerf profile from a single scan with different laser cutting parameters at three positions along sample measured using scanning microscope - (a) 1.75 kW at 6 m/s; (b) 1.75 kW at 8 m/s; (c) 2 kW at 6 m/s; (d) 2 kW at 8 m/s, respectively.

1 to 5. The maximum value of 5 can be assigned when the quality of kerf is optimal with negligible burr, for the burr analysis, and perfect kerf depth uniformity between top, middle and bottom of the scanned area, for the uniformity analysis. The number 5, in this analysis, can be assigned when the number of scans to complete a full cutting is equal or lower than 4. The three parameters are weighted differently as following: uniformity factor 1.2; burr factor 1.1; scans factor 1. These factors are chosen based on the consideration that the uniformity and burr of the cutting are more important than the cycle time for this proposed work. The authors decided to weight the uniformity by 20% more and burr analysis by 10% more with respect to the number of scans. The results are proposed in TABLE II.

Power [kW]	Speed [m/s]	Uniformity	Burr	Scans	Total
1.75	6	3	3	5	11.9
1.75	8	3	3	4	10.9
2	6	4	4	5	14.2
2	8	4	4	4	13.2

TABLE II: Criteria matrix - weight factor for uniformity 1.2; weight factor for burr 1; weight factor for scans 1.

Analysing the results of the criteria matrix, the best trade-off between uniformity, burr and number of scans results to be the settings P = 2 kW, S = 6 m/s, getting a total score of 14.2. Therefore, those are selected as the best cutting settings for the proposed methodology.

B. Full cutting

Several samples of NO20 material are fully cut using the selected laser set point P = 2 kW S = 6 m/s. As expected, four beam scans were enough to fully cut through the material. The single strip dimensions are width = 30 mm, length = 240 mm, thickness = 0.20 mm. The top surface of one sample is shown in Fig. 3. Those samples are cut with different idle times between beam scans from 0 ms to 1 s with a step of 100 ms. The results suggest that idle time has no impact on the kerf cutting quality for the proposed material and sample geometry.

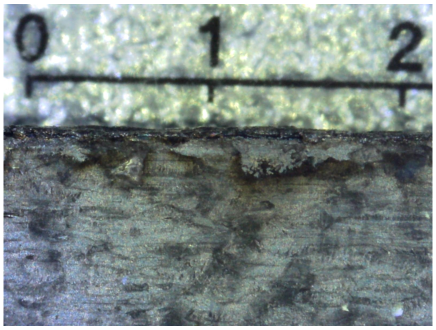

Fig. 3: Kerf analysis for the sample cut with P = 1.75 kW, S = 6 m/s, and IT = 1 s captured by a commercial microscope.

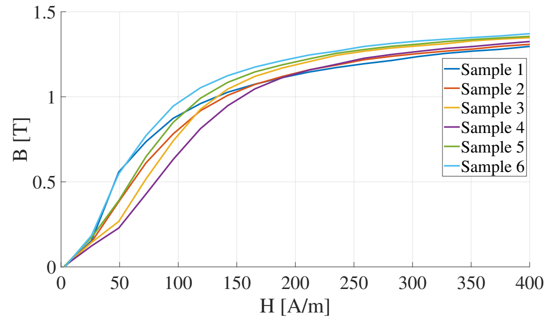

Fig. 4: Repeatability analysis on 6 samples cut by remote fibre laser with settings of P=2 kW, S=6 m/s and IT=0 s - DC BH curves.

IV. Magnetic properties degradation

A characterisation of NO20 magnetic properties was performed using a Laboratorio Elettrofisco AMH-1K-S permeameter, which is carried out for different samples using the selected point (P = 2 kW, S = 6 m/s) and several idle times. A repeatability analysis shows the lack of consistency in the samples when it comes to the material magnetic performance. Therefore, outputs were averaged across six samples for each setting in order to obtain a better statistical average. The idle times between 500 ms and 1 s and between 0 s and 50 ms are not further investigated due to the negligible differences between the two values on the magnetic performance. As mentioned in section II-B, the idle time needs to be added to the cutting time to have the effective time between scans. For the proposed single strip shape geometry, with dimension of 240 mm x 30 mm, and selected cutting speed of 6 m/s, the time to complete a full path is 136 ms. This includes acceleration/decelerations of the galvanometer and was measured by the laser control software.

A. Remote fibre laser repeatability

This section analyses the repeatability for the remote fibre laser cutting. Fig. 4 shows the BH curves for 6 samples which were cut in rolling direction and with the same laser setting of P = 2 kW, S = 6 m/s, and IT = 0 s. It is possible to appreciate that the curves present a marked difference with respect to each other, even using the same laser setting. It means that the remote laser is not consistent, although it has not been possible to identify a possible reason for the variation. Therefore, an analysis using 6 samples for each setting is performed.

B. Average analysis on different samples

This section proposes a BH curve analysis for several idle times using the average of six samples that were cut by remote laser at a power of P = 2 kW and speed of S = 6 m/s. The selected idle times are the same proposed in section IV-A analysis: 0 s, 50 ms, 100 ms, 200 ms, 300 ms, 400 ms, 500 ms and 1 s. Fig. 5 shows a trend as the shorter is the idle time the higher is the damage, in the linear zone of the curve. This trend is not valid for knee and quasi-saturation regions. The linear zone analysis does not show any benefits, in terms of magnetic

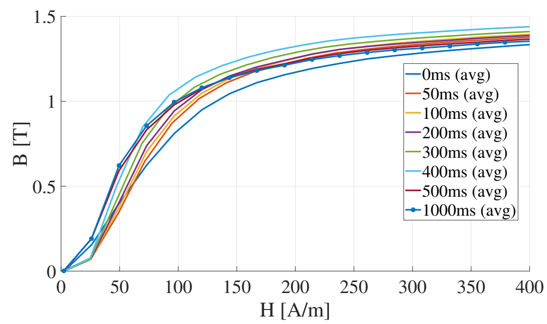

Fig. 5: Averaged DC BH curve of six single NO20 lamination strips for the different idle times between beam scans.

properties, for the idle time of 1000 ms with respect to the 500 ms. Apart the initial part of the linear zone, and considering the full curve, the IT = 400 ms results in the best flux density performances. The corresponding relative permeabilities for all idle times are shown in Fig. 6.

A deeper investigation is proposed on the following three magnetic field strength points, H = 50 A/m (linear zone), H = 120 A/m (next to the knee point), and H = 400 A/m (quasi-saturation region) to compare the corresponding flux density values for all six strips for each of the following idle times: 0 s, 50 ms, 100 ms, 200 ms, 300 ms, 400 ms, 500 ms, 1 s. Fig. 7a focuses on the linear zone, showing a higher flux

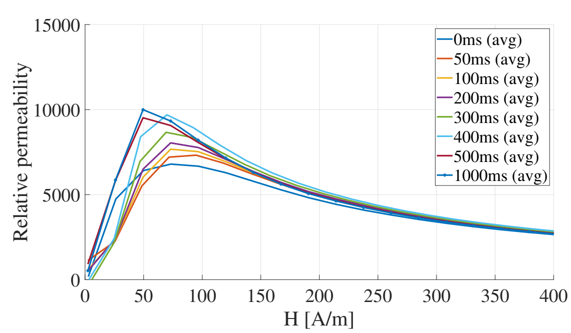

Fig. 6: Averaged relative permeability of six single NO20 lamination strips for the different laser idle times between beam scans.

density value for longer idle times in the interval between 200 ms and 500 ms. After 500 ms, the flux density reaches a plateau keeping its maximum value. For idle times lower than 200 ms, the flux density values are similar and lower than for longer idle times. Fig. 7b displays the trend flux density vs idle time at the knee region. It shows a trend of higher flux density values for longer idle times for the range 0 s - 400 ms. Above 400 ms, it is possible to see a decrement in the flux density values. Fig. 7c presents the trend between flux density and idle times in the quasi-saturation region, showing a similar trend to that at the knee region. The idle time impact on the flux density at the knee and saturation regions results to be counter-intuitive. Indeed, a longer idle time should result in lower HAZ, and in turn lower magnetic degradation. The lack of repeatability and the flux density/idle time curve need further investigations, for example grain structure and temperature analyses. In addition, it is possible to appreciate that the interval of flux density values for the same settings are more marked in the linear zone than in the knee and quasi-saturation regions. By contrast, consistency in the EDM cutting method is higher, with a variation of only 5.4% in the flux density value between samples.

Considering those analyses and the overall cutting time, the idle time of 400 ms is the best choice for fully cutting the NO20 material with power 2 kW and speed 6 m/s.

C. Comparison of cutting methods

This section compares the best selected remote laser cutting parameters (P = 2 kW, S = 6 m/s, IT = 400 ms), guillotine and EDM cutting methods in terms of BH curves and relative permeability. Measurements were averaged over three samples produced by guillotine methodology, and six samples produced by laser and EDM techniques. This was done because the guillotine technique showed a high level of repeatability. The EDM cutting was performed with the following machine settings: servo feed (no load speed) of 1.00 inch/min, servo voltage of 40 V, wire tension of 1600 grams, wire speed of 0.25 meters per min. It is worth highlighting that those settings were not optimised for cutting NO20 laminations. The BH curves comparison is shown in Fig. 8, where it is possible to see that the remote laser technique presents a higher flux density value in the quasi-saturation region with respect to the guillotine and EDM methods. On the other hand, the laser technique achieves the lower performance in the linear zone, reaching the knee point for higher values of magnetic field strength. The relative permeability (see Fig. 9) is higher up to H = 100 m/s for guillotine and EDM techniques. After H = 100 A/m, the relative permeability is very similar for guillotine, EDM and laser methods. Based on this analysis, it is possible to affirm that remote fibre laser cutting, with appropriate settings, can result in comparable magnetic performances with respect to EDM and guillotine methods, presenting even better performance in quasi-saturation region.

D. Linear region analysis with improved resolution

This subsection presents the averaged DC BH curves analyses of section IV-B and IV-C, focusing on the linear zone

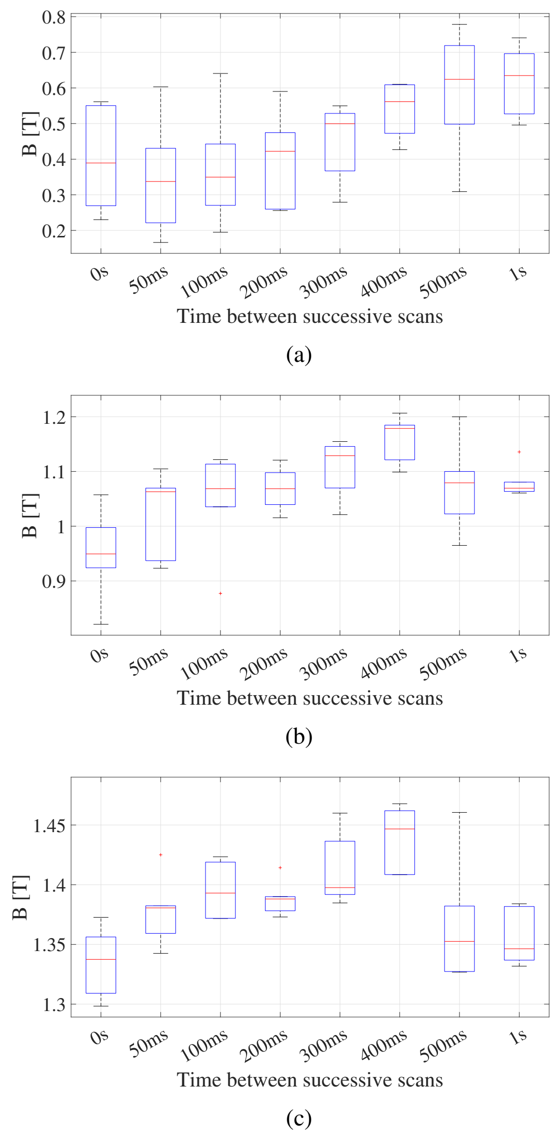

Fig. 7: Repeatability analysis on 6 samples for different idle times: (a) H=50 A/m - (b) H=120 A/m - (c) H=400 A/m. Centre (red) line indicates median; bottom and top of boxes indicate 25 and 75th percentiles; and whiskers indicate range of data.

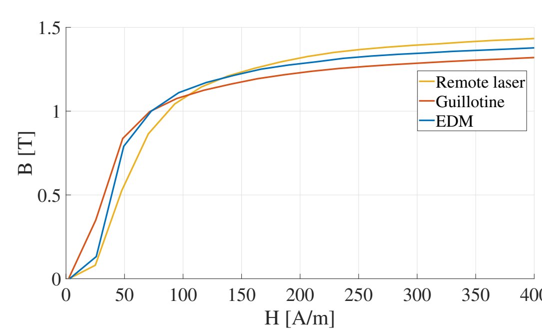

Fig. 8: Averaged DC BH curve comparison between the optimum remote laser settings, guillotine and EDM method NO20 lamination cuttings.

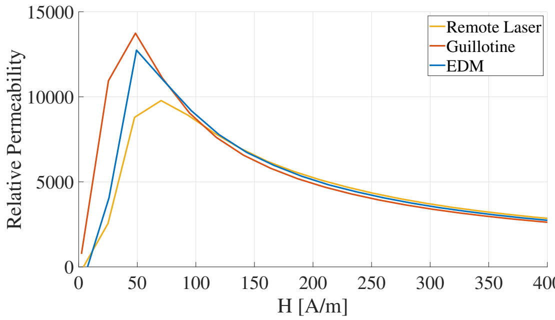

Fig. 9: Averaged relative permeability comparison between the optimum laser settings, EDM and guillotine method NO20 lamination cuttings

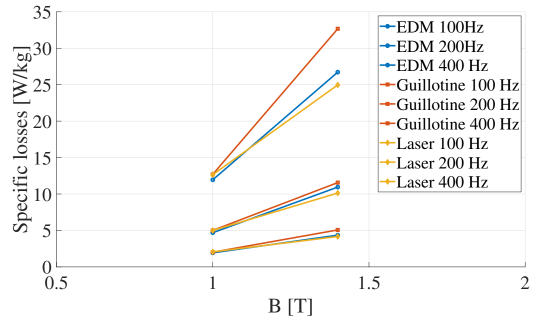

Fig. 12: Comparison of specific losses between guillotine (average of 3 samples), EDM (average of 6 samples), and remote laser with selected settings (average of 6 samples).

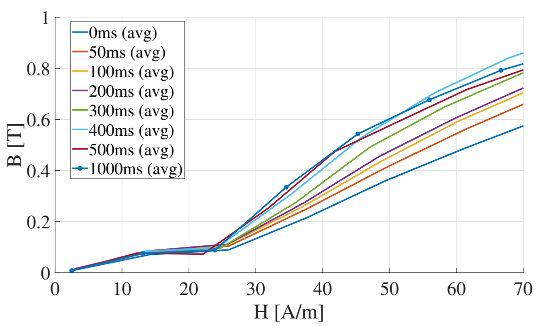

Fig. 10: Averaged DC BH curve of six single NO20 lamination strips for the different idle times between beam scans - linear zone.

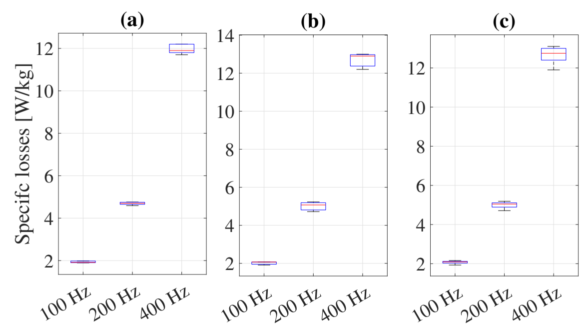

Fig. 13: Specific losses analysis at 1T - (a) EDM method, (b) guillotine method, (c) remote laser method. Centre (red) line indicates median; bottom and top of boxes indicate 25 and 75th percentiles; and whiskers indicate range of data.

and improved test resolution. The permeameter was set with a voltage step of 0.01 V instead of 0.02 V which was used for the full range BH curve zones presented in the previous subsections. Fig. 10 and Fig. 11 show the linear zone with an improved resolution for both remote laser cutting for the different idle times and the selected remote laser settings against guillotine and EDM methods. The improved resolution analysis confirms the same trend in the linear zone compared to the lower resolution and full BH curve range analysis.

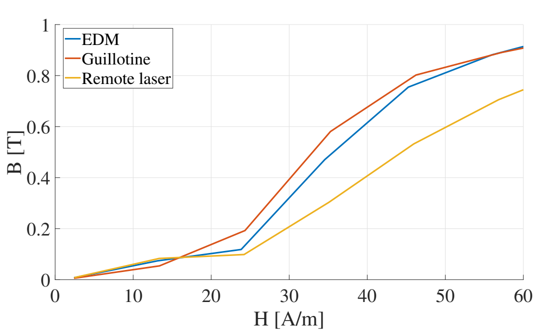

Fig. 11: Averaged DC BH curve comparison between the optimum remote laser settings, guillotine and EDM methods for NO20 cuttings - linear zone.

E. AC losses analysis

This section compares the losses generated by the different cutting methods proposed in this article. Fig. 12 shows the comparison of specific losses against the flux density at 100 Hz, 200 Hz and 400 Hz. It can be seen that at 1 T the losses are very similar between the different cutting methods for all the frequencies under investigation. In contrast, there is a marked difference between these methods at 1.4 T, in particular at 400 Hz, where the remote laser presents the best results showing lower losses by 6.5% with respect to EDM, and 25.8% with respect to guillotine, with the latter having the worst performance. Specific losses sensitivity analyses are shown in Fig. 13 and Fig. 14 for both 1 T and 1.4 T for all the samples and frequencies under investigation. It is possible to appreciate that all boxes are very small, meaning that the measurements were similar each other. It is worth highlighting that the specific loss values, which generate the boxes, are the average of three different measurements for each sample and test. Those three measurements have a maximum difference lower than 3% between each other.

V. Conclusion

This article proposed a methodology to select good remote laser settings for cutting non-oriented silicon NO20 laminations. The baseline point was selected by performing microscopy analysis on single scans, made by different power and

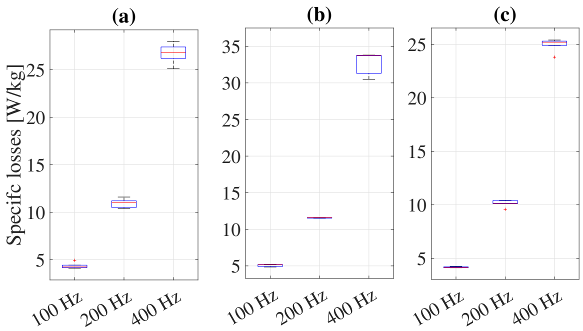

Fig. 14: Specific losses analysis at 1.4T - (a) EDM method, (b) guillotine method, (c) remote laser method. Centre (red) line indicates median; bottom and top of boxes indicate 25 and 75th percentiles; and whiskers indicate range of data.

speed laser settings. Using the selected optimum power and speed laser settings, full cuts were performed with different idle times between scans. The optimum idle time setting was selected by characterising the material magnetic properties by permeameter on the full cut samples. The analysis shows a clear impact of the idle time on the material magnetic properties. The main issue for laser cutting is the lack of consistency in terms of impact on material magnetic properties in which the performance can vary significantly, even using the same settings. In this regard, an average analysis approach was used to study the impact of remote laser cutting on the material magnetic properties. This approach is appropriate for electrical machine applications in which the rotor, if the required speed is not high, and stator are created from a stack of laminations. Finally, a comparison between remote laser, guillotine, and EDM techniques was performed, showing that an appropriate selection of laser settings can result in contained degradation of the performance in linear zone, higher flux density values in the quasi-saturation region and lower losses for the material cut by remote laser than guillotine and EDM methods for the proposed case study. This is an important statement considering that the EDM method is commonly used as benchmark due to the minimal impact on the magnetic proprieties. Even if the optmised EDM cutting could potentially perform better than remote laser, this work showed that the remote laser can be considered a valid option, if its settings are carefully selected, considering the losses, performance, and shorter cutting time. Further investigation is needed for a better understanding of the flux density/idle time trend and the lack of consistency for the remote laser.

References

[1] A. Krings, M. Cossale, A. Tenconi, J. Soulard, A. Cavagnino and A. Boglietti, ”Magnetic Materials Used in Electrical Machines: A Comparison and Selection Guide for Early Machine Design,” in IEEE Industry Applications Magazine, vol. 23, no. 6, pp. 21-28, Nov.-Dec. 2017, doi: 10.1109/MIAS.2016.2600721.

[2] A. Winter, L. Tinkler and G. W. Jewell, ”Remote laser cutting of high cobalt content electrical steel: preliminary results and microscopy,” 11th International Conference on Power Electronics, Machines and Drives (PEMD 2022), Hybrid Conference, Newcastle, UK, 2022, pp. 708-711, doi: 10.1049/icp.2022.1141.

[3] Robert Baumann, René Siebert, Patrick Herwig, Andreas Wetzig, Eckhard Beyer; Laser remote cutting and surface treatment in manufacturing electrical machines—High productivity, flexibility, and perfect magnetic performance. J. Laser Appl. 1 February 2015; 27 (S2): S28002. https://doi.org/10.2351/1.4906383

[4] M Emura, F.J.G Landgraf, W Ross, J.R Barreta, The influence of cutting technique on the magnetic properties of electrical steels, Journal of Magnetism and Magnetic Materials, Volumes 254–255, 2003, Pages 358-360, ISSN 0304-8853, https://doi.org/10.1016/S0304-8853(02)00856-9.

[5] Andreas Wetzig, Robert Baumann, Patrick Herwig, René Siebert, and Eckhard Beyer ”Laser remote cutting of metallic materials: opportunities and limitations”, Proc. SPIE 9657, Industrial Laser Applications Symposium (ILAS 2015), 965708 (1 July 2015); https://doi.org/10.1117/12.2175507

[6] Pihlava, A., Purtonen, T., Salminen, A. et al. Quality aspects in remote laser cutting. Weld World 57, 179–187 (2013). https://doi.org/10.1007/s40194-012-0004-4

[7] A. Wagner, M. Lütke, A. Wetzig, L. M. Eng; Laser remote-fusion cutting with solid-state lasers. J. Laser Appl. 1 November 2013; 25 (5): 052004. https://doi.org/10.2351/1.4816651

[8] R. Sundaria, D. G. Nair, A. Lehikoinen, A. Arkkio and A. Belahcen, ”Effect of Laser Cutting on Core Losses in Electrical Machines—Measurements and Modeling,” in IEEE Transactions on Industrial Electronics, vol. 67, no. 9, pp. 7354-7363, Sept. 2020, doi: 10.1109/TIE.2019.2942564.

[9] F. Martin, U. Aydin, R. Sundaria, P. Rasilo, A. Belahcen and A. Arkkio, ”Effect of Punching the Electrical Sheets on Optimal Design of a Permanent Magnet Synchronous Motor,” in IEEE Transactions on Magnetics, vol. 54, no. 3, pp. 1-4, March 2018, Art no. 8102004, doi: 10.1109/TMAG.2017.2768399.

[10] C. -C. Chiang et al., ”Effects of Annealing on Magnetic Properties of Electrical Steel and Performances of SRM After Punching,” in IEEE Transactions on Magnetics, vol. 50, no. 11, pp. 1-4, Nov. 2014, Art no. 8203904, doi: 10.1109/TMAG.2014.2329708.

[11] R. Sundaria, A. Lehikoinen, A. Arkkio and A. Belahcen, ”Effects of Manufacturing Processes on Core Losses of Electrical Machines,” in IEEE Transactions on Energy Conversion, vol. 36, no. 1, pp. 197-206, March 2021, doi: 10.1109/TEC.2020.2999528.